Life Sciences 229 (2019) 139–148

Contents lists available at ScienceDirect

Life Sciences

journal homepage: www.elsevier.com/locate/lifescie

Anti-hyperalgesic and anti-inflammatory effects of citral with β-cyclodextrin and hydroxypropyl-β-cyclodextrin inclusion complexes in animal models

Caio A. Campos[a], Bruno S. Lima[a], Gabriela G.G. Trindade[a], Eloísa P.B.S.S. Souza[a], Débora S.A. Mota[b], Luana Heimfarth[b], Jullyana S.S. Quintans[b], Lucindo J. Quintans-Júnior[b], Eliana M. Sussuchi[c], Victor H.V. Sarmento[d], Flávio M.S. Carvalho[e], Ricardo N. Marreto[f], Roseane M.R. Costa[g], Rogéria S. Nunes[a], Adriano A.S. Araújo[a,*], Saravanan Shanmugam[a,*], Parimelazhagan Thangaraj[h]

[a] Department of Pharmacy, Federal University of Sergipe, São Cristovao, SE, Brazil
[b] Department of Physiology, Federal University of Sergipe, São Cristovao, SE, Brazil
[c] Department of Chemistry, Federal University of Sergipe, São Cristóvão, SE, Brazil
[d] Department of Chemistry, Federal University of Sergipe, Itabaiana, SE, Brazil
[e] Department of Mineralogy and Geotectonics, University of São Paulo, São Paulo, SP, Brazil
[f] Faculty of Pharmacy, Federal University of Goiás, Goiânia, GO, Brazil
[g] Faculty of Pharmacy, Federal University of Pará, Belém, PA, Brazil
[h] Department of Botany, Bharathiar University, Coimbatore, Tamil Nadu, India

ARTICLE INFO

Keywords:
Citral
Cyclodextrins
Inclusion complexes
Anti-hyperalgesic
Anti-inflammatory

ABSTRACT

Citral (CIT) is a monoterpene formed by the geranial and neral stereoisomers. CIT is the major compound of *Cymbopogon citratus* essential oil, commonly known as "lemongrass", and has demonstrated potential anti-hyperalgesic, anti-nociceptive and anti-inflammatory effects. However, CIT shows high volatility, low solubility in water and consequent low bioavailability, which limits its use. Therefore, the aim of this study was to evaluate cell viability, anti-hyperalgesic and anti-inflammatory effects of inclusion complexes of CIT on β-cyclodextrin (β-CD) and hydroxypropyl-β-cyclodextrin (HP-β-CD). Initially, physical mixture (PM) and freeze-dried inclusion (FD) complexes of CIT/β-CD and CIT/HP-β-CD were obtained in the molar ratio (1:1). The samples were characterized by DSC, TG/DTG, FT-IR, XRD, SEM and the complexation efficiency were performed by HPLC. Cell viability assay was performed by rezasurin reduction technique in J774 macrophages cell line. The motor activity through rota rod apparatus, mechanical hyperalgesia and pleurisy induced by carrageenan were evaluated in mice. The complexation of CIT was evidenced with β-CD and HP-β-CD by the characterization techniques analyzed. The complexation efficiency of CIT/β-CD and CIT/HP-β-CD were 78.6% and 71.7%, respectively. The CIT, CIT/β-CD and CIT/HP-β-CD showed cell viability in macrophages and did not interfere in the motor activity of mice. Besides that, the samples demonstrated antihyperalgesic and anti-inflammatory activity due to the reduction in total leukocytes and TNF-α levels. However, CIT/β-CD has better pharmacological effects among the three samples evaluated. Therefore, CIT/β-CD has potential for the development of products to treat inflammatory and pain reactions.

1. Introduction

Pain is one of the four cardinal signs of inflammation defined by Celsus during the 1st century CE. Pain mediation occurs through nociceptors, which are specialized subsets of sensory neurons that closely associate with peripheral tissues such as the skin, joints, respiratory tract, and gastrointestinal tract. Nociceptors can respond to mechanical, chemical or thermal stimuli [1,2,61]. Acute inflammatory pain is one of the painful conditions, which is characterized by hypernociception caused by sensitization of primary nociceptors, also called hyperalgesia or allodynia [3,4,62].

A significant part of the world's population is affected by some type of pain, causing loss of quality of life [5,6]. The treatments for painful conditions, such as inflammatory pain, are often unsatisfactory, since

* Corresponding authors.
E-mail addresses: left.ufs@hotmail.com, adriasa2001@yahoo.com.br (A.A.S. Araújo), saranflora04@gmail.com (S. Shanmugam).

https://doi.org/10.1016/j.lfs.2019.05.026

Available online 11 May 2019

their etiology is heterogeneous and the pathophysiological mechanisms are complex [7,8]. Nonsteroidal anti-inflammatory drugs (NSAIDs) are usually prescribed for this type of condition, however, these usually have relevant side effects such as GI ulcer and cardiotoxicity *etc.* Also, NSAIDs are relatively safer and effective to treat inflammatory pain but they are not very effective to treat neuropathic pain [9,10]. Therefore, new therapeutic alternatives for the treatment of inflammatory pain have been investigated. In this context, molecules derived from natural products have promising effects and offer the possibility of developing new drugs with greater efficacy and performance in inflammatory pain [11,12].

Citral (CIT) is a monoterpene formed by the neral (cis-citral) and geranial (trans-citral) stereoisomers, considered the major compound of the essential oil obtained from the leaves of *Cymbopogon citratus* plant species, popularly known as lemongrass [13]. CIT demonstrated anti-inflammatory effect through the inhibition of inducible nitric oxide synthase (iNOS) and nuclear factor kappa B (NF-κB) [14] and inhibit the pro-inflammatory interleukins IL-1β and IL- 6 [15]. Also, CIT has synergistic anti-inflammatory effect with naproxen [16], including antinociceptive and anti-inflammatory effect when administered intraperitoneally in rodents [7]. Further, reduction of acute nociceptive stimulus without causing motor dysfunction, reduction of mechanical hyperalgesia, and significant gastroprotective action against ulcers induced by non-steroidal anti-inflammatory drugs [17,63]. In addition, CIT has been reported as a partial agonist of potential transient receptors type 1 (TRPV1), which reinforces its analgesic and anti-inflammatory activity [18]. However, its practical use is limited due to its low solubility in water, because it is a hydrophobic compound, and due to its low stability to environmental agents such as oxygen and elevated temperatures, being highly volatile [19].

Cyclodextrins (CDs) have been widely used to improve the bioavailability of the natural products, such as terpenes and essential oils, for their pharmacological application, thus enhancing analgesic and anti-inflammatory profiles [20]. CDs are cyclic oligosaccharides in the form of truncated cones, composed of α-D-glucopyranose monomers linked by α-1,4 bonds, the natural CDs being classified as α-CD, β-CD or γ-CD, having six, seven or eight monomers, respectively. They have a hydrophobic central cavity and a hydrophilic surface and can incorporate a variety of molecules to form host-guest complexes [21,22], resulting in increased water solubility, stability and bioavailability of the guest molecule [23,24]. Among natural CDs, β-cyclodextrin (β-CD) is mostly used for drug complexation, however, its use is restricted by its low aqueous solubility. Also, β-CD is nephrotoxic and it makes its use limited clinically. That's why other derivatives such as hydroxypropyl, sulfobutylether-beta-cyclodextrin are developed. [25]. Some chemical modifications have been made on natural CDs to overcome the limiting extent of solubility, optimize their capacity in specific applications, or to provide them with new features. The replacement of the hydrogen atoms of the β-CD hydroxyl groups by 2-hydroxypropyl groups, resulting in hydroxypropyl-β-cyclodextrin (HP-β-CD), represents perhaps the most widely used chemical modification. Compared with natural ones, the main characteristic of this modified CD is greater aqueous solubility. As for pharmaceutical applications, its advantages are increased solubility, dissolution rate, and bioavailability of the drug [26].

In the perspective of retaining the therapeutic potential and improving the solubility and stability properties of CIT, by preparation of promising the inclusion complexation of CDs. Therefore, the aim of this study was to prepare the CIT inclusion complexes with β-CD and HP-β-CD. Also, the characterization, evaluate cell viability *in vitro* and the anti-hyperalgesic and anti-inflammatory activities *in vivo* for the CIT inclusion complexes.

2. Materials and methods

2.1. Chemicals

CIT (purity ≥95%), carrageenan and tween 80 was purchased from Sigma Aldrich (USA). β-CD and HP-β-CD (purity ≥95%) were purchased from Wacker Chemie AG. Triton X-100, Dulbecco Modified Eagle Medium (DMEM), Resazurin sodium salt were purchased from Sigma Chemical Co., St. Louis, MO (USA) and fetal bovine serum (FBS) was obtained from Gibco BRL (USA).

2.2. Preparation of samples

The samples were prepared based on molecular weight of CIT (152.23 $g.mol^{-1}$), β-CD (1134.98 $gmol^{-1}$) and HP-β-CD (1375.37 gmol-1), with a molar ratio of 1:1 (CIT/β-CD or HP-β-CD) by methods of physical mixture (PM) and freeze drying (FD). The PM sample was prepared by the addition of CIT to an agate mortar containing β-CD or HP-β-CD powder under manual stirring, which were then stored in sealed glass containers [27]. The FD sample was prepared by addition of CIT and β-CD or HP-β-CD to 20 mL of distilled water, this solution was submitted to agitation by a magnetic stirring device at 400 rpm (Quimis Q 261A21, Brazil) at room temperature for 36 h and then it was frozen at −20 °C for 24 h and freeze-dried by lyophilization. Thereafter, the prepared sample was stored in airtight glass containers. This method of preparation was adapted from Carvalho et al., 2017 [28].

2.3. Characterization of the complex

2.3.1. Thermal analysis

The Differential Scanning Calorimetry (DSC) and Thermogravimetric (TG/DTG) curves were obtained in the temperature range of 25 to 500 °C and 25 to 600 °C, respectively, using Shimadzu DSC-60 and TGA-60 instruments, under dynamic nitrogen atmosphere (l00 $ml.min^{-1}$) and a temperature range of 10 $°C.min^{-1}$ utilizing aluminum (DSC) and platinum (TG/DTG) crucibles with approximately 2 mg of the sample. The instruments were previously calibrated and/or verified using the standard calcium oxalate for TG (purity 99.99%) and indium metal for DSC.

2.3.2. Karl Fischer titration

The moisture contents of CIT, β-CD, HP-β-CD and their PM and FD samples were determined through the Karl Fischer Titrino Plus KF 870 method (Metrohm).

2.3.3. Fourier transform infrared spectroscopy (FT-IR)

The infrared spectra of CIT, β-CD, HP-β-CD and their PM and FD samples were obtained in the range from 4000 to 400 cm^{-1} in KBr pellets using a Varian 640-IR Fourier Transform spectrophotometer at room temperature.

2.3.4. X-ray diffractometry (XRD)

The X-ray diffraction of β-CD, HP-β-CD and their PM and FD samples were obtained in Siemens model D5000 equipment, with CuKα tubes, in the range of 5 to 50° (2θ) and 1 s at each step.

2.3.5. Scanning electron microscopy (SEM)

The morphology of samples of CIT, β-CD, HP-β-CD and their respective PM and FD were analyzed in a scanning electron microscope (JEOL JSM-6060, Tokyo, Japan) operating at 7 kV. For this analysis, the samples were gold-sputtered.

2.4. Complexation efficiency (CE%)

The inclusion efficiency of CIT in the inclusion complexes were determined by the ultrasonic-centrifugal method [29]. The amount of

CIT into inclusion complexes were analyzed by HPLC. HPLC analysis was carried out using the high-performance liquid chromatography system that consisted of a degasser DGU-20A3, two LC-20 CE pumps, a SIL-20A HT auto injector, CTO-20A column oven, SPDM20Avp photodiode array detector (DAD) and a CBM-20A system controller (Shimadzu® Co., Kyoto, Japan). Chromatographic analysis was performed on a Phenomenex® C18 analytical column (4.6 × 250 mm, 5 μm) placed in a column oven set at 25 °C. The solvents used to the mobile phase were: (A) ultrapure water and (B) acetonitrile. The mobile phase flow rate was 1.0 mL/min and sample injection volume was 20 μL. The elution profile consisted of isocratic mode (40:60 - A/B - v/v) during 10 min of analysis. Detector was set at 233 nm for acquiring chromatograms. CIT stock solution (1 mg/mL) was prepared and the standard curve was obtained with five different concentrations in the linear concentration range of 5–150 μg/ml. The samples were prepared and analyzed in triplicate ($n = 3$).

HPLC analysis was used to determine CIT content entrapped in β-CD and HP-β-CD. Therefore, 5 mg of CIT/β-CD and CIT/HP-β-CD inclusion complex was dissolved in 5 ml of acetonitrile and the solutions obtained were submitted to agitation by a magnetic stirring device operating at 250 rpm at room temperature for 24 h, to allow enough time for all entrapped active compound to be in solution. Then, the solutions was centrifuged at 3200 *g* for 30 min to remove the β-CD and HP-β-CD, leaving only active compound. The supernatant was collected, filtered on membrane filters (PTFE - 0.45 μm) and analyzed by HPLC. The samples were prepared and analyzed in triplicate ($n = 3$). The complexation efficiency (CE%) of CIT in β-CD and HP-β-CD calculated using Eq. (1). The calibration curve of CIT concentration was $y = 146{,}175\times + 1346.2$ ($R^2 = 0.9992$).

$$CE\ (\%) = \frac{mass\ of\ recovered\ CIT\ in\ inclusion\ complex}{mass\ added\ CIT\ in\ inclusion\ complex} \times 100 \quad (1)$$

where “mass of recovered” is the quantified amount of CIT in the solid inclusion complexes and “mass added” is the amount of CIT initially used to prepare the inclusion complexes.

2.5. Cell viability

To evaluate cell viability, the resazurin reduction technique (Alamar Blue Assay) was used. Cells of the J774 lineage were cultured in an incubator at 37 °C and 5% CO 2 in flasks containing Dulbecco Modified Eagle Medium (DMEM) supplemented with fetal bovine serum 10%. Cells were trypsinized and plated in transparent 96-well plates. After the adhesion period of 24 h, the following treatments were added: CIT and FD of CIT/β-CD and CIT/HP-β-CD at concentrations 10, 50, 100 μg/mL. Two hours before the end of the 72 h incubation period, resazurin diluted in 0.15 mg/mL PBS was added to a final concentration 75 μg/mL in each well. Triton-X 100 (TX) (0.5%) was used as the negative control, and cells with DMEM 10% FBS were used as the positive control (PC). The resazurin reaction time was 2 h, and the estimated number of cells in each well on the day of reading was 2×10^5 cells.

The assay was performed in triplicate ($n = 3$) and the readings were performed by absorbance on the SpectraMax® M5 endpoint reader at wavelengths $\lambda = 570$ nm and 595 nm, and the quantification method was used according to the methodology described by Al-Nasiry et al., 2007 [30].

2.6. Animals

Adult (2 to 3 months old) male Swiss mice (28–32 g) were randomly housed in appropriate cages at 23 ± 2 °C with a 12-h light: dark cycle (light from 06:00 to 18:00), with free access to food and tap water. All experiments were carried out between 09:00 am and 02:00 pm in a quiet room. Experimental protocols were approved by the Animal Care and Use Committee at the Federal University of Sergipe (CEPA/UFS #52/17).

2.7. Carrageenan-induced pleurisy

Adult male Swiss mice (28–32 g) were divided into four groups ($n = 6$, per group) treated with vehicle (Saline 0.9%, p.o), CIT (100 mg/kg, dissolved in vehicle and tween 0.2%, p.o), and FD of CIT/HP-β-CD (100 mg/kg, p.o) or CIT/β-CD (100 mg/kg, p.o), 60 min before carrageenan pleural injection. Pleurisy was induced in the mice by intrapleural administration of 100 μL of 1% (w/v) carrageenan suspension in sterile saline solution [31]. An adapted 13 × 5 needle was introduced into the right side of the thoracic cavity for injection of the carrageenan solution. Four hours after the induction of pleurisy, the animals were euthanized, and the pleural inflammatory exudate was collected through pleural lavage with 1 mL of PBS containing ethylenediaminetetraacetic acid (EDTA; 10 mM). The exudate volume was centrifuged (1500 rpm, 10 min), and the supernatant was collected for the determination of cytokines levels in the pleural fluid. The cells were ressuspended in 1000 μl PBS and an aliquot of 10 μL was diluted with Turk's solution (1:20). The total leukocytes were counted in a Neubauer chamber, examining four external quadrants, using a light microscope [32].

2.8. Determination of TNF-α in the pleural fluid

Tumor necrosis factor alpha (TNF-α) in the pleural cavity was assessed 4 h after the injection of carrageenan. TNF-α was quantified on supernatant free of cells by ELISA following the manufacturer's protocol (BD-Bioscience Pharmingen, San Diego, CA).

2.9. Hyperalgesia induced by carrageenan

The hyperalgesia protocol was performed as in the previous report [33]. The Adult male Swiss mice (28-32 g) were divided into four groups ($n = 6$, per group) and treated with vehicle (Saline 0.9%, p.o), CIT (100 mg/kg, dissolved in vehicle and tween 0.2%, p.o), and FD of CIT/HP-β-CD (100 mg/kg, p.o) or CIT/β-CD (100 mg/kg, p.o). Sixty minutes after the treatment, 20 μL of carrageenan (300 μg/paw) were injected subcutaneously into the subplantar region of the hind paw. The mechanical hyperalgesia was evaluated at 30, 60, 120 and 180 min after the hyperalgesic agent injection.

2.10. Mechanical hyperalgesia measurement

Mechanical hyperalgesia was tested in mice as per previous report [33], using a digital analgesiometer (digital Von Frey; Insight®, São Paulo, Brazil). In a quiet room, the mice were placed in acrylic cages (12 × 10 × 17 cm) with wire grid floors for 15–30 min before the test. The investigator was trained to apply the tip perpendicularly to the central area of the hind paw with a gradual increase in pressure. The end was characterized by the withdrawal of the paw followed by clear flinching movements. After this response, the pressure intensity was automatically recorded. The intensity of stimulus was obtained by averaging three measurements taken with minimal intervals of 3 min. The animals were tested before and after the treatment.

2.11. Evaluation of the motor activity (Rota rod)

To investigate if the treatments could influence the motor activity of the animals and consequently impair the assessment of the nociceptive behavior in the experimental tests, the motor activity of the animals was evaluated in a rota rod apparatus, according to Dunham & Miya [34] with some modifications. Initially, the mice able to remain on the rota rod apparatus (AVS®, Brazil) longer than 180 s (7 rpm) were selected 24 h before the test. Then the selected animals were divided into five groups ($n = 6$) and treated with vehicle (saline 0.9%, p.o), CIT (100 mg/kg, dissolved in vehicle and tween 0.2%, p.o), FD of CIT/HP-β-CD (100 mg/kg, p.o), FD of CIT/β-CD (100 mg/kg, p.o) and diazepam

(DZP, 1.5 mg/kg, i.p). Each animal was tested on the rota rod and the time (s) they remained on the bar for up to 180 s was recorded 0.5, 1 and 2 h after administration.

2.12. Statistical analysis

Data were analyzed by one-way ANOVA followed by Tukey's test using GraphPad Prism software (GraphPad, San Diego, CA). Further, in the mechanical hyperalgesia, we have used the two-way ANOVA followed by Bonferroni's test. The values were expressed as the mean ± Standard Error of the Mean (SEM) and differences with $p < 0.05$ were considered significant.

3. Results and discussion

3.1. Thermal analysis and Karl Fischer titration

Thermal methods are widely used in the characterization of CDs and their complexes, mainly because of the speed of analysis. Among them, we have used the DSC. The formation of inclusion complexes can be identified in the profiles of the DSC curves by the reduction, disappearance or displacement of endothermic or exothermic peaks and by the relevant variations in enthalpy of the pure or complex drug [35,36].

In Fig. 1A the DSC curves of CIT, β-CD, HP-β-CD, PM/β-CD, FD/β-CD, PM/HP-β-CD, FD/HP-β-CD are presented. The CIT DSC curve showed an endothermic peak at 155 °C relative to its volatilization and decomposition. The β-CD curve showed an endothermic event between 27 and 102 °C, characteristic of the water loss of the molecule, an event between 216 and 225 °C for phase transition, and an endothermic event between 298 and 360 °C related to the sample decomposition. Similar results related to the DSC curve of β-CD were obtained by Quintans et al., 2016 [37] which reported that the Hecogenin acetate (HA) and β-CD produced a significant antinociceptive ($p < 0.01$) profile and also decreased mechanical hyperalgesia, with HA-β-CD showing significantly better effects when compared to HA alone ($p < 0.05$). In the FD/β-CD curve, a reduction of intensity in the event related to water loss is observed, comparing with the β-CD curve, which is still less intense than the PM/β- CD, which may indicate replacement of water molecules in the β-CD cavity by CIT molecules by the FD method, a phenomenon that usually occurs in the formation of inclusion complexes which was proved previously, the complete disappearance of the characteristic endothermic peak of sulfamerazine in the inclusion complexes indicating a strong interaction of the drug with CD nanocavities and the stable encapsulated complexes are formed between sulfamerazine and CDs [38]. In the FD/β-CD curve, shift of the melting and degradation event were observed, which showed 297.9–323.89 °C on β-CD followed by PM displayed 313.47–342.52 °C at 311 °C, and FD exhibited 316.21–348.55 °C. Further, HP-β-CD and its PM, FD inclusion complex revealed 304.8–325.9 °C, 317.27–389.58 °C and 329.98–386.09 °C respectively. All these results indicates the higher thermal stability of FD, which is characteristic of the formation of inclusion complexes [35]. Thus, the observed results suggest interaction and complexation between CIT and β-CD by the FD method is better than another complexation.

The HP-β-CD curve showed an endothermic event between 26 and 79 °C relative to water loss of the molecule and an endothermic event between 303 and 373 °C related to its melting and degradation. Both in the PM/HP-β-CD DSC curve and in the FD/HP-β-CD curve, a shift of the melting and degradation event observed on the HP-β-CD curve was observed, but a greater shift in the curve of the FD. Similar phenomena were also observed and described by Kfoury et al., 2014 [39], when analyzing the DSC curve of the β-pinene/HP-β-CD complex. This indicates a higher thermal stability of the FD sample, characteristic of inclusion complex formation.

TG thermal analyzes for inclusion complexes with CDs are often used in combination with DSC analyzes to support and aid in the interpretation of DSC results. TG allows to determine changes in sample weight in relation to temperature change. The comparison of the TG

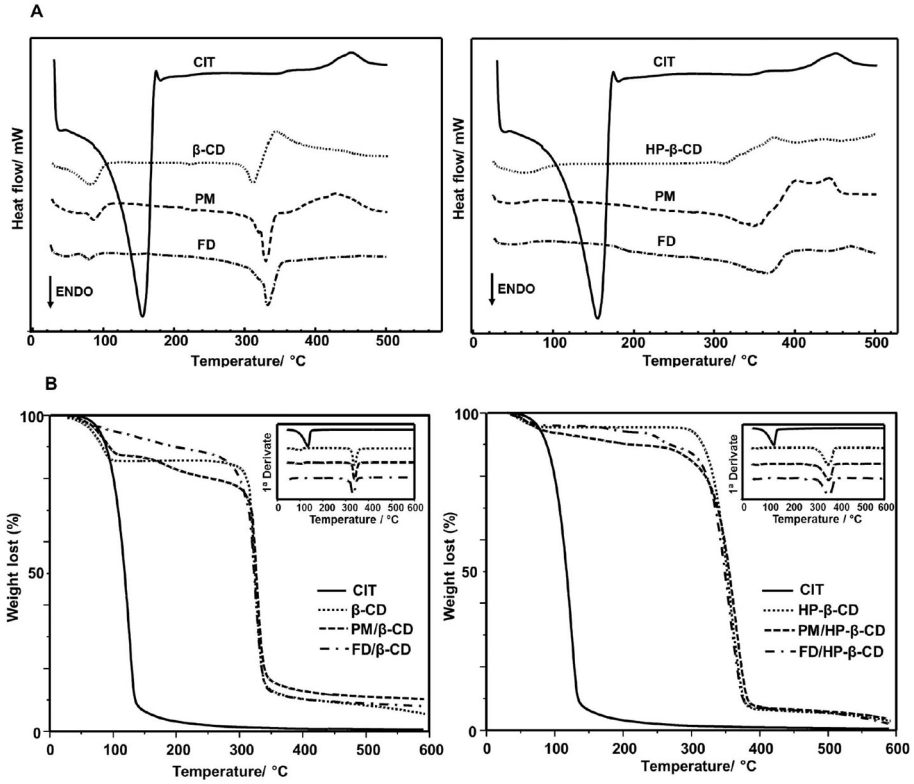

Fig. 1. DSC (A) and TG/DTG curves (B) of CIT, β-CD, HP-β-CD, PM/β-CD, FD/β-CD, PM/HP-β-CD, FD/HP-β-CD samples in dynamic nitrogen atmosphere (100 ml.min-1) and heat 10 °C.min-1.

Table 1
Percentage of weight loss and degradation temperature obtained from TG/DTG curves and water content obtained by Karl Fischer method.

Samples	Δm_1 (%) (25–200 °C)	Δm_2 (%) (200–400 °C)	Δm_3 (%) (400–600 °C)	Degradation temperature (°C)	H_2O (%)
CIT	98.56	0.65	0.88	131.30	0.47
β-CD	13.64	74.52	14.19	326.06	14.44
PM/β-CD	12.73	73.78	13.02	328.32	13.59
FD/β-CD	9.76	78.76	10.17	330.59	10.69
HP-β-CD	5.27	84.43	5.84	359.52	9.57
PM/HP-β-CD	9.16	83.12	6.92	360.63	9.33
FD/HP-β-CD	7.43	89.35	7.51	363.76	7.98

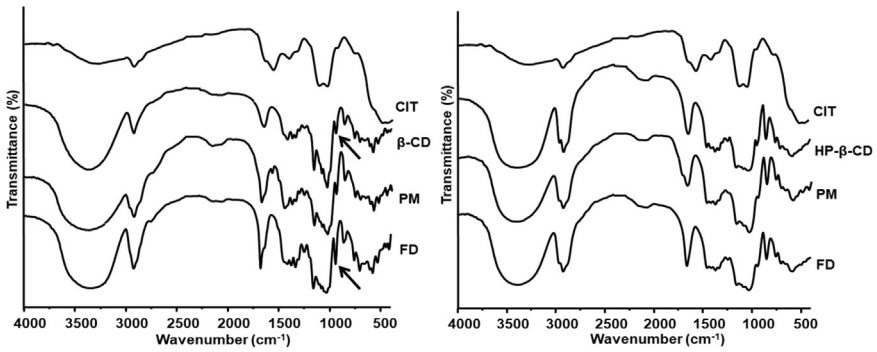

Fig. 2. FT-IR spectrum of CIT, β-CD, HP-β-CD, PM/β-CD, FD/β-CD, PM/HP-β-CD, FD/HP-β-CD samples.

curves of pure components, physical mixture and inclusion complex should show changes in the mass loss profile of the supposed complex, being indicative of interactions between the components and/or formation of a true inclusion complex [35].

The TG/DTG curves of the samples are shown in Fig. 1B, and percentages of mass loss and moisture determination by Karl Fischer are shown in Table 1. As can be seen in Fig. 1B and Table 1, the CIT TG curve presented a fast and intense mass loss profile with a $\Delta m = 98.56\%$ in the first temperature range (25–200 °C), related to its volatilization and decomposition. The β-CD and HP-β-CD TG curves presented three stages of mass loss: a first step of $\Delta m = 13.64\%$ for β-CD and $\Delta m = 4.48\%$ for HP-β-CD (25–200 °C) referring to the water release of the molecule [41], in which approximate values were obtained by Karl Fischer analysis (14.44% and 9.57%, respectively), which is specific method for determination of water content. They presented a step with $\Delta m = 74.52\%$ for β-CD and $\Delta m = 84.43\%$ for HP-β-CD, between 200 and 400 °C, demonstrating greater mass loss in this temperature range, and mass losses of 14.19% and 5.48%, respectively, between 400 and 600 °C, having in this range the occurrence of a continuous carbonization process. β-CD showed degradation temperature of 326.06 °C and HP-β-CD of 359.52 °C.

As shown in Table 1, the methods of obtaining the two CDs presented values of Δm in the first stage quite close to their respective values of water content determined by Karl Fischer. In the first stage of mass loss, a lower loss of FD/β-CD and FD/HP-β-CD were observed when compared to PM/β-CD and PM/HP-β-CD, which may indicate a smaller amount of water in the CD cavity, resulting from possible complexation and substitution of the water molecules present in the cavity, by hydrophobic molecules of the CIT [40]. In the FD/β-CD and FD/HP-β-CD methods, larger losses of mass were observed in the second stage, compared to the losses of PM/β-CD and PM/HP-β-CD, which can be explained since in this step there is still CIT due to FD complexation, which reinforces a higher interaction and stability between the components (CIT and CDs) in this second stage temperature range. To further confirm the results, higher degradation temperatures were observed in FD/β-CD and FD/HP-β-CD compared to each of the pure CDs and CIT, which indicates higher thermal stability, thus suggesting complexation of CIT with β-CD and HP-β-CD by the FD method.

Karl Fischer titration is a good tool for the evaluation of water concentration in CDs and inclusion complexes and the results of this titration are related to TG results. The Karl Fischer titration method is more accurate than TG because it evaluates only water concentration and, in addition, the “surface” and “tightly bound” water molecules can be determined [40].

3.2. Fourier transform infrared spectroscopy (FT-IR)

FT-IR is widely used to characterize the solid systems with CDs, for being able to present fast and precise determinations. The phenomena involved in the complexation make the deviations and changes of intensity of the bands corresponding to the chemical groups of the drug or CD very subtle, requiring a careful interpretation of the data [36].

The FT-IR spectra of CIT, β-CD, HP-β-CD, PM/β-CD, FD/β-CD, PM/HP-β-CD, FD/HP-β-CD are shown in Fig. 2. The CIT spectrum showed a band at 2924 cm^{-1} referring to the axial deformation vibrations of CH groupings, a band at 1681 cm^{-1} related to the C=O group of aldehydes, a band at 1409 cm^{-1} related to angular strain vibrations of CH_2 groups, a 1358 cm^{-1} band for angular deformations of CH_3 groups, and absorption bands between 1090 and 706 cm^{-1} for C–H and C–C bonds.

The FT-IR spectrum of β-CD showed an absorption band between 3681 and 3067 cm^{-1} relative to the OH group vibrations, a band at 2933 cm^{-1} related to CH groups and a band at 1645 cm^{-1} also related to OH groups. The bands present in 1426, 1366, 1332 and 1255 cm^{-1} regions of the spectrum refer to the CH stretches, those located at 1164 and 1028 cm^{-1} are related to the C–O groups of ethers and hydroxyls and the bands lying between 1000 and 700 cm^{-1} refer to the C–H and C–C bonds of the glucopyranose ring skeleton. Similar results of FT-IR spectrum of β-CD were obtained by Menezes et al., 2014 [29]

The HP-β-CD FT-IR spectrum showed a prominent wavelength absorption band between 3679 and 3078 cm^{-1} referring to the vibrations of O–H groupings, one band at 2927 cm^{-1} related to C–H groups and one band at 1642 cm^{-1} referring to O–H groups. The band present at the wavelength between 1470 and 1251 cm^{-1} of the spectrum refer to the C–H stretches, the bands at 1160 and 1029 cm^{-1} are related to the C–O groups of ethers and hydroxyls and the bands lying between 1000

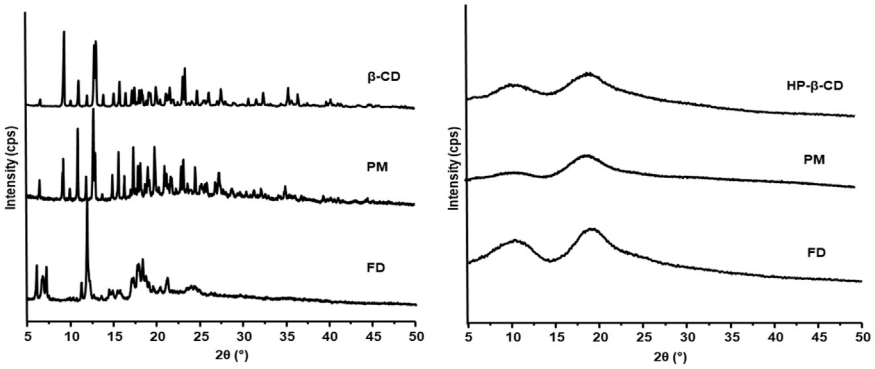

Fig. 3. X-ray diffractograms of β-CD, HP-β-CD, PM/β-CD, FD/β-CD, PM/HP-β-CD and FD/HP-β-CD.

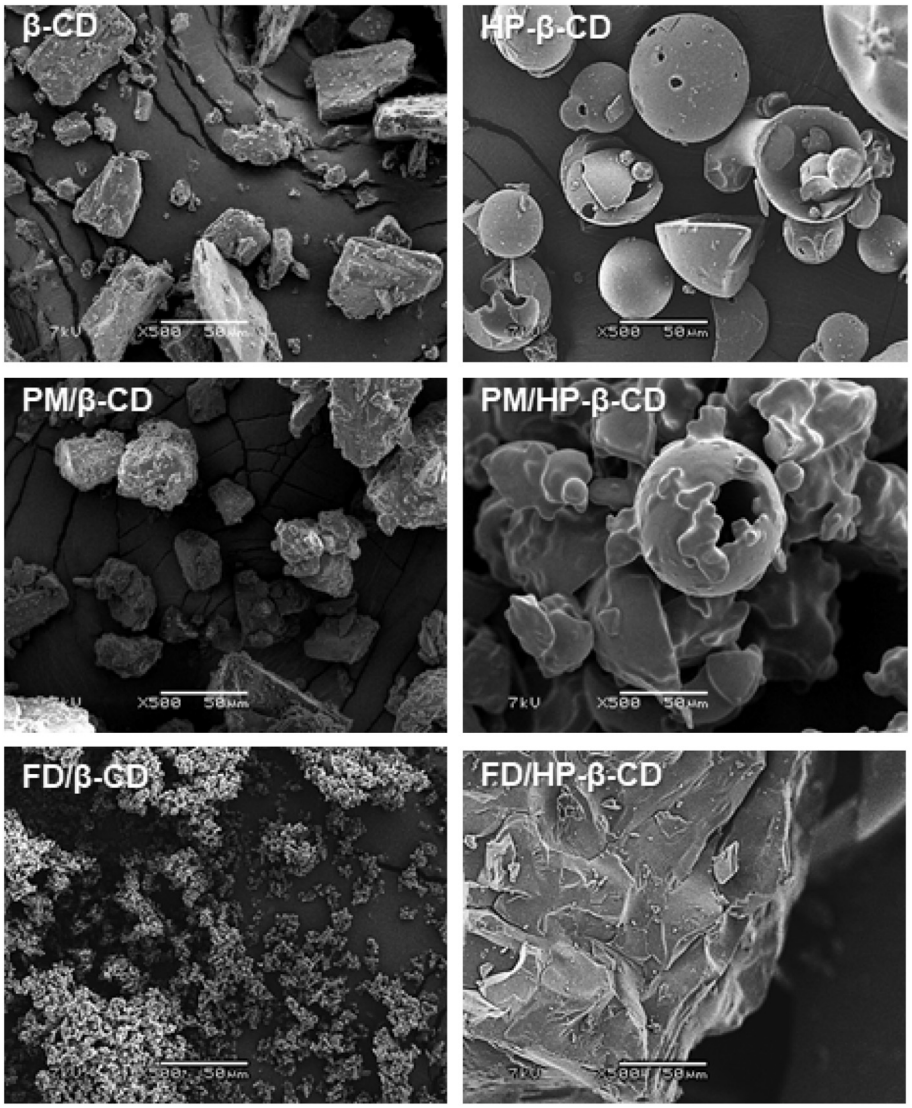

Fig. 4. SEM micrographs of β-CD, HP-β-CD, PM/β-CD, FD/β-CD, PM/HP-β-CD and FD/HP-β-CD (500×).

and 700 cm^{-1} refer to the C—H and C—C connections. Similar results were obtained by Jug. Becirevic-Lacan, 2004 [42]

Very similar profiles of β-CD and HP-β-CD were observed in the FT-IR spectra of PM/β-CD and PM/HP-β-CD, respectively. A similar profile of HP-β-CD was observed in the FD/HP-β-CD spectrum, but when the FD/β-CD spectrum was observed, is perceived a band shift and increase of 936 cm^{-1} in the β-CD spectrum, being observed in 941 cm^{-1} in the FD spectrum, and with greater intensity. This phenomenon suggests complexation, as was also observed and described by Menezes et al., 2016 [43].

3.3. X-ray diffractometry (XRD)

The XRD technique is widely used to quickly identify unknown

crystalline substances, as well as to determine the degree of crystallinity or amorphization of the samples examined [35]. Differences in the samples, such as appearance or disappearance of peaks or changes in relative intensities, are indications of complex formation [44].

In Fig. 3 the X-ray diffractograms of β-CD, HP-β-CD, PM/β-CD, FD/β-CD, PM/HP-β-CD and FD/HP-β-CD are represented. The β-CD diffraction lines presented at the angles of 2θ 9.33°, 10.50°, 12.91° and 23.05° demonstrate their crystalline profile, also seen and described in a similar way by Menezes et al., 2016 [43]. The FD/β-CD method showed changes in the crystallinity profile of β-CD, which was seen by the reduction of the number of peaks, suggesting the formation of a sample with an amorphous characteristic and consequently more soluble in water. On the other hand, PM/β-CD did not present changes in the crystallinity profile of β-CD, thus suggesting formation of inclusion complex between CIT and β-CD by the FD method.

The HP-β-CD diffractogram showed an amorphous profile, also described by Pose-Vilarnovo et al., 2001 [45]. The two methods (PM/HP-β-CD and FD/HP-β-CD) demonstrated a diffraction profile without crystalline peaks, such as HP-β-CD, which may be justified by the fact that CIT is a liquid and volatile compound. However, in FD/HP-β-CD an increase in the signal intensity regarding diffraction has been observed, and this may indicate inclusion complex formation, as was also demonstrated by Zhu et al., 2016 [46] and Pose-Vilarnovo et al., 2001 [45]. These phenomena was also demonstrated earlier likely XRD results were in well concord with those obtained by DSC to confirm the encapsulation of compounds with CDs in the solid state [38].

3.4. Scanning electron microscopy (SEM)

SEM allows an in-depth investigation of the morphological aspects of the raw materials and their corresponding physical mixtures and inclusion complexes obtained by different preparation methods. Although this technique is inadequate to evaluate the true formation of the inclusion complex, it helps to show morphological alterations that may be related to the interactions between the components, thus indicating a possible complexation [35].

The SEM images of β-CD, HP-β-CD, PM/β-CD, FD/β-CD, PM/HP-β-CD and FD/HP-β-CD are presented in Fig. 4 at resolutions of 500×. The particles of the β-CD presented morphology of square and rectangular crystals was also observed by Carvalho et al., 2017 [28]. In the PM/β-CD sample the β-CD particles were still observed without alteration of the morphology, which indicates that no interaction occurs through this method, but when the FD/β-CD was observed, a reduction in size of the particles and amorphization was perceived, characteristics that indicate the formation of inclusion complex, due to changes in the crystalline morphology of β-CD. HP-β-CD particles exhibited spherical vesicle morphology, as also described by Moyano et al., 1994 [47]. In the PM/HP-β-CD photomicrographs, a cluster of particles is observed, although the presence of HP-β-CD spherical vesicles is observed, indicating that there is no interaction or complexation by this method. In FD/HP-β-CD, plaque formation was observed, with a total change in HP-β-CD particle morphology. This phenomenon indicates formation of inclusion complex and was also described by Yang et al., 2013 [48]. All these characterization studies reveals the inclusion complex of the compound CIT effectively act with the cyclodextrin molecules and improve their host-guest interaction. Further, this complexation might play a vital role in the pharmacological activities of the particular compound which might improve the bioavailability nature.

3.5. Complexation efficiency (CE%)

The CE is a quantitative parameter to determine the amount of active compound entrapped in the inclusion complexes and was calculated using Eq. (1) as listed in Table 2. PM method for CIT/β-CD obtained a CE of 1.32% and for CIT/HP-β-CD showed a CE of 2.65%, evidencing any interaction of CIT with CDs studied for this method.

Table 2
Complexation efficiency (CE) values of PM and FD (CIT/β-CD) and (CIT/HP-β-CD) inclusion complexes using HPLC at 233 nm.

Samples	Methods	CE (%)*
CIT/β-CD	PM	$1.32^{a} \pm 0.87$
	FD	$78.60^{b} \pm 1.53$
CIT/HP-β-CD	PM	$2.65^{c} \pm 0.55$
	FD	$71.66^{d} \pm 0.47$

* The results were expressed as mean ± SD of three replicate samples ($n = 3$) of the analyzes; and entrapment efficiency (CE) values with differing superscript letters indicate $p < 0.05$ significant.

However, the highest percentages were obtained for FD method and showed a CE of 78.60% (CIT/β-CD) and 71.66% (CIT/HP-β-CD), proving that CIT was complexed with efficiency in the β-CD cavity. This can be related to the chemical structure and physical properties, the type of interaction between CIT and β-CD and the procedure used to prepare the inclusion complexes (Ref 1). Dou et al., 2018 [49] obtained a complexation efficiency of 72.30% for thymol in β-CD inclusion complexes prepared by the FD method, which was significantly lower than this present study (Table 2). The authors also reported that this much complexation efficiency of thymol in β-CD inclusion complexes produces antifungal activity against the *Geotrichum citri-aurantii.* In this present result, CIT/β-CD inclusion complex by FD procedure show significant complexation efficiency results, which corroborates with characterization results also could influence the compounds for the further pharmacological activities.

3.6. Cell viability

The J774 macrophage lineage was chosen for the cell viability assay because it is like human macrophages, which considered as the first cell line of immune defense in addition to being distributed throughout the organism and widely used in biological assays [50]. Thus, it is important that formulations intended for oral administration are tested in that assay and do not cause cytotoxicity. From the Alamar Blue assay it was possible to measure the cellular viability of macrophages J774 based on the ability to reduce resazurin in resofurin, property is related to its metabolic activity.

In Fig. 5 are presented the percentages of reduction of the

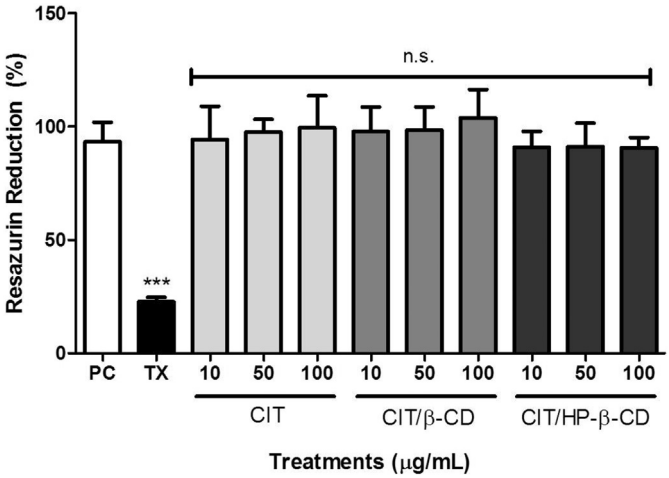

Fig. 5. Cell viability assay by the reduction of resazurin in cells of the J774 lineage. TX: Triton-X 100, PC: cells in untreated DMEM medium, CIT: citral, CIT/β-CD: inclusion complex citral with β-cyclodextrin, CIT/HP-β-CD: inclusion complex citral with hydroxipropil-β-cyclodextrin, n.s.: non- significant. Incubation time 72 h. $n = 3$, triplicate. ANOVA one-way followed Tukey post-test. ***$p < 0.001$ when compared to the other groups.

rezasurina (%) generated by the samples. Maintenance of cell viability of cells in DMEM (PC) medium, as expected, and reduction of cell viability of the cells in the TX medium was observed. The other treatments with CIT, CIT/β-CD and CIT/HP-β-CD concentrations showed levels comparable to the positive control, showing no significant difference between them and in relation to the PC, in addition, all were statistically different from the wells treated with TX 100. The TX 100 is widely used as control in tests and cell toxicity because it is a surfactant that smooths the cell's phospholipid membrane, causing the non-viable cells to be unable to reduce resazurin and allowing its use as a cell death control [51].

Resazurin reduction assays for CIT were used in toxicity studies against *Trypanosoma brucei* and *Leishmania amazonenses*. In these cases, the essential oils of plants were used in which the CIT was identified as a component. The alamar blue assay has this dual function, which can be used both to measure the toxicity of a formulation against a pathogen or tumor cells, and serve as an indication that the formulation can be safe in the treatment of patients, such as Ijaz et al. (2016) [52] who used this assay to assess the toxicity of cyclodextrins to a mucoadhesive vaginal delivery system for acyclovir.

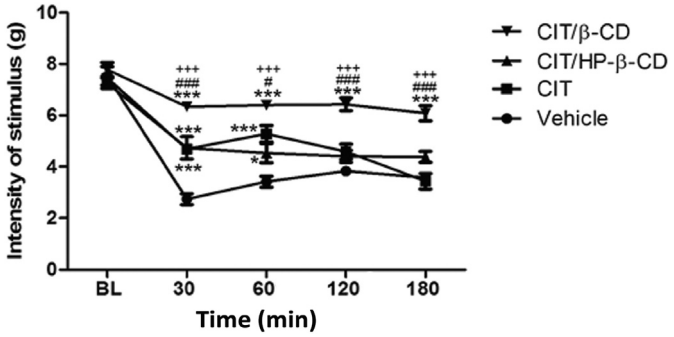

Fig. 7. Effect of CIT alone or complexed in hyperalgesia induced by carrageenan in hind paw of mice. Animals were treated with vehicle, citral (CIT, 100 mg/kg, p.o), citral complexed in hydroxypropyl-β-cyclodextrin (CIT/HP-β-CD, 100 mg/kg, p.o) or citral complexed in β-cyclodextrin (CIT/β-CD, 100 mg/kg, p.o) 60 min before injection of carrageenan. The evaluation occurred 30, 60, 120 and 180 min after carrageenan injection. ANOVA one-way followed Tukey's test (n = 6/group). *$p < 0.05$ or ***$p < 0.001$ when compared to the vehicle. #$p < 0.05$ or ###$p < 0.001$ when compared to the CIT/HP-β-CD. + + +$p < 0.001$ when compared to the CIT.

3.7. Carrageenan-induced pleurisy and determination of TNF-α in the pleural fluid

In pleurisy induced by carrageenan, the administration of carrageenan into the pleural space of mice induces an inflammatory process with increase in total leukocyte count and upregulated the TNF-α production in pleural fluid [53]. Treatment with CIT (100 mg/kg p.o.), CIT/HP-β-CD (100 mg/kg p.o.) or CIT/β-CD (100 mg/kg p.o.) provoked a significant decrease in total leukocyte count and caused a significant reduction in TNF-α levels in pleural fluid when compared to the vehicle group (Fig. 6)

To evaluate the anti-inflammatory effect of CIT, we performed the carrageenan-induced pleurisy assays. In pleurisy acute inflammatory model, we observed fluid extravasation, leukocyte infiltration and several biochemical parameters involved in the inflammatory response [53,54]. Our findings show that CIT, CIT/β-CD and CIT/HP-β-CD inhibited the cell influx induced by carrageenan. This effect is associated to inhibition of proinflammatory cytokines TNF-α production. Song et al. (2016) [55] have described that citral has anti-inflammatory activity which can be attributed to decreased NF-κB activation and decreased production of inflammatory mediators such as TNF-α. They also suggest TNF-α upregulate the expression of VCAM-1 and ICAM-1 and the compound citral dose-dependently inhibited VCAM-1 and ICAM-1 expression in LPS-stimulated HUVEC cells. Based on this report our research also acts with the same mechanism and inhibit the production of TNF-α production. Also, the inclusion complexation of CIT and cyclodextrins might plays a vital role to improve the solubility and bioavailability which is also response for the reduction of the TNF-α production.

3.8. Hyperalgesia induced by carrageenan

In hyperalgesia induced by carrageenan, CIT presented anti-hyperalgesic effect at 30 ($p < 0.001$) and 60 min ($p < 0.001$) after induction. Likewise, CIT/HP-β-CD reduced hyperalgesia at the time of 30 ($p < 0.001$) and 60 min ($p < 0.05$). Interestingly, the animals treated with CIT/HP-β-CD showed a significant reduction of hyperalgesia at all moments of evaluation ($p < 0.001$) when compared to the control. In addition, CIT/β-CD also showed a significant difference when compared to CIT-treated animals (p < 0.05 and p < 0.001) and CIT/HP-β-CD (p < 0.001) (Fig. 7).

Hyperalgesia is one of the most common signs of an inflammatory disorder and injection of carrageenan into a mice hind paw leads to thermal hyperalgesia, providing a model to evaluate the ability of compounds to alleviate this response [56]. In addition, pro-

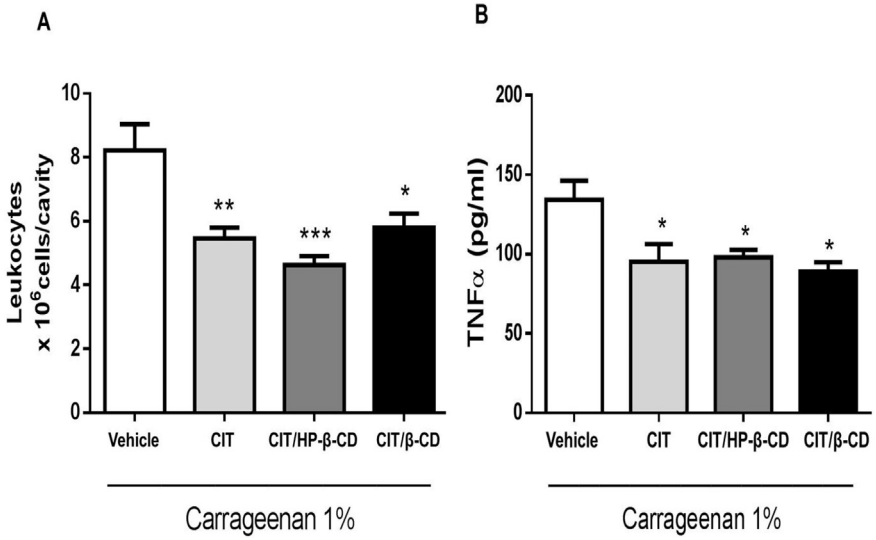

Fig. 6. Effect of CIT alone or complexed on leukocyte migration into the pleural cavity induced by carrageenan in mice (A), and on TNF-α levels (B). Groups of mice were pre-treated with vehicle, citral (CIT, 100 mg/kg, p.o), citral complexed in hydroxypropyl-β-cyclodextrin (CIT/HP-β-CD, 100 mg/kg, p.o) or citral complexed in β-cyclodextrin (CIT/β-CD, 100 mg/kg, p.o). Each value represents the mean ± SEM. Asterisks denote statistical significance, *$p < 0.05$, **$p < 0.01$ and ***$p < 0.001$ related to control group. ANOVA followed by Tukey's test ($n = 6$, per group).

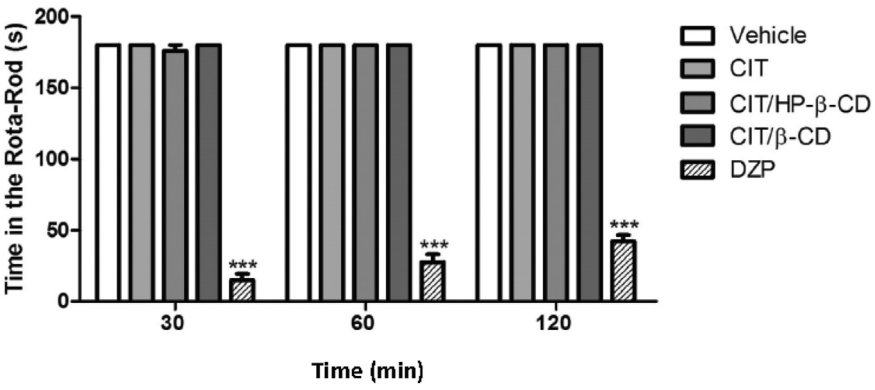

Fig. 8. Effect of CIT alone or complexed on motor coordination of mice. Animals were treated with vehicle, citral (CIT, 100 mg/kg, p.o), citral complexed in hydroxypropyl-β-cyclodextrin (CIT/HP-β-CD, 100 mg/kg, p.o), citral complexed in β-cyclodextrin (CIT/β-CD, 100 mg/kg, p.o) or diazepam (DZP, 1.5 mg/kg, i.p) 30, 60 and 120 min before evaluation. ANOVA two-way followed Bonferroni's test ($n = 6$/group). ***$p < 0.001$ when compared to the vehicle.

inflammatory cytokines, such as TNF-α, have been implicated with the pathophysiology of inflammatory pain [57,58]. So, the inhibitory effect on TNF-α production are associated to anti-hyperalgesia profile of CIT. These findings agree with Nishijima et al., 2014 [17] that reported the anti-nociceptive effects of CIT in different pain models. Also, oral pre-treatment with HA or HA-CD produced a significant antinociceptive ($p < 0.01$) profile and also decreased mechanical hyperalgesia, with HA-β-CD showing significantly better effects when compared to HA alone ($p < 0.05$). The hypothesis of HA acting *via* the descending pain-inhibitory mechanisms is reinforced by the Fos protein expression [37]. Moreover, the complexation of CIT with β-CD improved the analgesic effect of CIT by the same mechanism and keeping its action for longer time than pure CIT. Cyclodextrins have been shown to be a useful tool to improve several pharmacological properties of non-polar compounds [59,60].

3.9. Evaluation of the motor activity (Rota rod)

When investigating the motor activity, the result show that none of the treatments could alter the motor coordination when compared to the control group, validating the anti-hyperalgesic effect of CIT/β-CD. The positive control diazepam could reduce the residence time of the animals on the rota rod (Fig. 8). Effect of HA or HA/β-CD complex (20 mg/kg, p.o.) on the rota-rod test also did not produce significant motor abnormalities in the earlier reported study [37]. Further, from the present study CIT/β-CD complexation also did not reveal any significant motor activity. These findings are consistent with the literature, showing that administration of the CIT/β-CD complexation can't reduce the grip strength of mice. From the results it could be proved that the CIT/β-CD complexation did not show any adverse effect to the animals like a side-effect of opioid drugs.

4. Conclusion

This present study was concluded that the inclusion complexes of CIT with β-CD and HP-β-CD, in the molar ratio of 1: 1, were obtained by the FD method, but that the complexing efficiency with the β-CD was higher (78.6%). CIT and CIT/β-CD and CIT/HP-β-CD complexes did not show cytotoxicity in J774 macrophages and demonstrated anti-inflammatory activity in mice according to the reduction of total leukocytes migration and TNF-α levels experiment by pleurisy model. Also, the anti-hyperalgesic effect of CIT/β-CD complex revealed statistically significant result when compared to CIT and CIT / HP-β-CD. Overall, the obtained result bare the complexation of CIT in β-CD have better profile of complexation when compared with HP-β-CD. Meanwhile, the same CIT in β-CD. Accordingly, the CIT in β-CD proves the efficiency in all biological activities it could be a better source for the pharmaceutical industries to develop new drugs for the treatment of human ailments.

Acknowledgments

This study was financially supported by the Conselho Conselho Nacional de Desenvolvimento Científico e Tecnológico – Brasil (CNPq), the Fundação de Apoio à Pesquisa e a Inovação Tecnológica do Estado de Sergipe (Fapitec/SE) - Brasil, the Coordenação de Aperfeiçoamento de Pessoal de Nível Superior - Brasil (CAPES - Finance Code 001).

Appendix A. Supplementary data

Supplementary data to this article can be found online at https://doi.org/10.1016/j.lfs.2019.05.026.

References

[1] F.A. Pinho-Ribeiro, W.A. Verri Jr, I.M. Chiu, Nociceptor sensory neuron–immune interactions in pain and inflammation, Trends Imunnol., 2016, doi:https://doi.org/10.1016/j.it.2016.10.001
[2] A.I. Basbaum, Cellular and molecular mechanisms of pain, Cell 139 (2009) 267–284.
[3] T.M. Cunha, W.A. Verri Jr., J.S. Silva, S. Poole, F.Q. Cunha, S.H. Ferreira, A cascade of cytokines mediates mechanical inflammatory hypernociception in mice, PNAS 102 (5) (2005) 1755–1760.
[4] M.J. Millan, The induction of pain: an integrative review, Prog. Neurobiol. 57 (1) (1999) 1–164.
[5] D.P. de Sousa, Analgesic-like activity of essential oils constituents, Molecules 16 (2011) 2233–2252.
[6] M.F. de Santana, A.G. Guimarães, D.N. Chaves, J.C. Silva, L.R. Bonjardim, W. de Lucca Júnior, J.N. de Souza Ferro, E.O. Barreto, F.E. Santos, M.B.P. Soares, C.F. Villarreal, J.S.S. Quintans, L.J. Quintans-Júnior, The anti-hyperalgesic and anti-inflammatory profiles of p-cymene: Evidence for the involvement of opioid system and cytokines, Pharm. Biol. 53 (11) (2015) 1583–1590.
[7] L.J. Quintans-Júnior, A.G. Guimarães, M.T. de Santana, B.E.S. Araújo, F.V. Moreira, L.R. Bonjardim, A.A.S. Araújo, J.S. Siqueira, A.R. Antoniolli, M.A. Botelho, J.R.G.S. Almeida, M.R.V. Santos, Citral reduces nociceptive and inflammatory response in rodents, Braz. J. Pharmacognosy 21 (3) (2011) 497–502.
[8] P.A. Batista, M.F.P. Werner, E.C. Oliveira, L. Burgos, P. Pereira, L.F. Silva Brum, G.M. Story, A.R. Santos, The antinociceptive effect of (-)-linalool in models of chronic inflammatory and neuropathic hypersensitivity in mice, J. Pain 11 (2010) 1222–1229.
[9] J.A. Mitchell, T.D. Warner, Cyclo-oxygenase-2: pharmacology, physiology, biochemistry and relevance to NSAID therapy, Br. J. Pharmacol. 128 (1999) 1121–1132, https://doi.org/10.1038/sj.bjp.0702897.
[10] R.O. Day, G.G. Graham, Non-steroidal anti-inflammatory drugs (NSAIDs), BMJ 346 (2013) f3195.
[11] T.K. Rabelo, A.G. Guimarães, M.A. Oliveira, J. Gasparotto, M.R. Serafini, A.A.S. Araújo, L.J. Quintans-Júnior, J.C.F. Moreira, D.P. Gelaina, Shikimic acid inhibits LPS-induced cellular pro-inflammatory cytokines and attenuates mechanical hyperalgesia in mice, Int. Immunopharmacol. 39 (2016) 97–105.
[12] C.R. McCurdy, S.S. Scully, Analgesic substances derived from natural products (natureceuticals), Life Sci. 78 (2005) 476–484.
[13] M. Katsukawa, R. Nakata, Y. Takizawa, K. Hori, S. Takahashi, H. Inoue, Citral, a component of lemongrass oil, activates PPARα and γ and suppresses COX-2 expression, Biochim. Biophys. Acta 1801 (2010) 1214–1220.
[14] C.T. Lin, C.J. Chen, T.Y. Lin, J.C. Tung, S.Y. Wang, Anti-inflammation activity of fruit essential oil from *Cinnamomum insularimontanum Hayata*, Bioresour. Technol. 99 (18) (2008) 8783–8787.
[15] T.F. Bachiega, J.M. Sforcin, Lemongrass and citral effect on cytokines production by murine macrophages, J. Ethnopharmacol. 137 (1) (2011) 909–913.
[16] M.I. Ortiz, M.P. González-García, H.A. Ponce-Monter, G. Castañeda-Hernández, P. Aguilar-Robles, Synergistic effect of the interaction between naproxen and citral

on inflammation in rats, Phytomedicine 18 (1) (2010) 74–79.
[17] C.M. Nishijima, E.G. Ganev, L. Mazzardo-Martins, D.F. Martins, L.R.M. Rocha, A.R.S. Santos, C.A. Hiruma-Lima, Citral: A monoterpene with prophylactic and therapeutic anti-nociceptive effects in experimental models of acute and chronic pain, Eur. J. Pharmacol 736 (2014) 16–25.
[18] S.C. Stotz, J. Vriens, D. Martyn, J. Clardy, D.E. Clapham, Citral sensing by transient receptor potential channels in dorsal root ganglion neurons, PLoS ONE 3 (2008) e2082.
[19] Wen-Chien Lu, Da-Wei Huang, Chiun-C.R. Wang, Ching-Hua Yeh, Jen-Chieh Tsai, Yu-Ting Huang, Po-Hsien Li, Preparation, characterization, and antimicrobial activity of nanoemulsions incorporating citral essential oil, J. Food Drug Anal. (2017) 1–8
[20] L.B. Rodrigues, A.O.B.P.B. Martins, J. Ribeiro-Filho, F.R.A.S. Cesário, F.F. Castro, T.R. de Albuquerque, M.N.M. Fernandes, B.A.F. da Silva, L.J. Quintans Júnior, A.A.S. Araújo, P.P. Menezes, P.S. Nunes, I.G. Matos, H.D.M. Coutinho, A.G. Wanderley, I.R.A. de Menezes, Anti-inflammatory activity of the essential oil obtained from *Ocimum basilicum* complexed with β-cyclodextrin (β-CD) in mice, Food Chem. Toxicol. (2017), https://doi.org/10.1016/j.fct.2017.02.027.
[21] G. Crini, Review: a history of cyclodextrins, Chem. Rev. 114 (21) (2014) 10940–10975.
[22] E. Pinho, M. Grootveld, G. Soares, M. Henriques, Cyclodextrins as encapsulation agents for plant bioactive compounds, Carbohydr. Polym. 101 (2014) 121–135.
[23] M.E. Brewster, T. Loftsson, Cyclodextrins as pharmaceuticals solubilizers, Adv. Drug Deliv. Rev. 59 (7) (2007) 645–666.
[24] M.M. Yallapu, M. Jaggi, S.C. Chauhan, Poly (beta-cyclodextrin) curcumin self-assembly: a novel approach to improve curcumin delivery and its therapeutic efficacy in prostate cancer cells, Macromol. Biosci. 10 (10) (2010) 1141–1151.
[25] D. Duchêne, D. Wouessidjewe, Physicochemical characteristics and pharmaceutical uses of cyclodextrin derivatives, Pharm. Techn. Int 2 (1990) 21–29.
[26] S. Concha-Santos, S. Pérez-Casas, P. Brocos, A. Piñeiro, Testing the effect of the cavity size and the number of molecular substitutions in host–guest complexes formed by 2-hydroxypropyl-cyclodextrins and n-octyl-β-D-glucopyranoside, J. Chem. Thermodyn. 67 (2013) 112–119.
[27] P.P. Menezes, M.R. Serafini, L.J. Quintans-Júnior, G.F. Silva, J.F. Oliveira, F.M.S. Carvalho, J.C.C. Souza, J.R. Matos, P.B. Alves, I.L. Matos, D.I. Ha, ˇdaˇrugaˇ, A.A.S. Araújo, Inclusion complex of (−)-linalool and b-cyclodextrin, J. Therm. Anal. Calorim. 115 (2014) 2429–2437.
[28] Y.M.B.G. Carvalho, P.P. Menezes, B.M.H. Sousa, B.S. Lima, I.A.S. Trindade, M.R. Serafini, E.W.M. Pereira, M.M. Rezende, J.S.S. Quintans, L.J. Quintans-Júnior, C.V. Nakamurac, E.F. Silva-Júnior, A.C. Crispim, T.M. Aquino, A.A.S. Araújo, Inclusion complex between β-cyclodextrin and hecogenin acetate produces superior analgesic effect in animal models for orofacial pain, Biomed. Pharmacother. 93 (2017) 754–762.
[29] L.E. Hill, C. Gomes, T.M. Taylor, Characterization of beta-cyclodextrin inclusion complexes containing essential oils (trans-cinnamaldehyde, eugenol, cinnamon bark, and clove bud extracts) for antimicrobial delivery applications, LWT Food Sci. Technol. 51 (1) (2013) 86–93, https://doi.org/10.1016/j.lwt.2012.11.011.
[30] S. Al-Nasiry, N. Geusens, M. Hanssens, C. Luyten, R. Pijnenborg, The use of Alamar Blue assay for quantitative analysis of viability, migration and invasion of choriocarcinoma cells, Hum. Reprod. 22 (5) (2007) 1304–1309.
[31] A.M. de Oliveira, L.M. Conserva, J.N. de Souza Ferro, F. de Almeida Brito, R.P. Lyra Lemos, E. Barreto, Antinociceptive and anti-inflammatory effects of octacosanol from the leaves of Sabicea grisea var. grisea in mice, Int. J. Mol. Sci. 13 (2012) 1598–1611.
[32] R. Vinegar, J.F. Truax, J.L. Selph, Some quantitative temporal characteristics of carrageenin-induced pleurisy in the rat, Proc. Soc. Exp. Biol. Med. 143 (1973) 711–714.
[33] T.M. Cunha, W.A.J. Verri, G.G, Vivancos, An electronic pressure-meter nociception paw test for mice, Braz. J. Med. Biol. Res. 37 (2004) 401–407.
[34] N.W. Dunham, T.S. Miya, A note on a simple apparatus for detecting neurological deficit in rats and mice, J. Am. Pharm. Assoc. Am. Pharm. Assoc. 46 (1957) 208–209.
[35] P. Mura, Analytical techniques for characterization of cyclodextrin complexes in the solid state: a review, J. Pharm. Biomed. Anal. 113 (2015) 226–238.
[36] M.A.M.A. Lyra, L.D.S. Fontes, D.A.F. Soares Sobrinho, J.L.P.J. Rolim Neto, Ferramentas analíticas aplicadas à caracterização de complexos de inclusão fármaco-ciclodextrina, Revista de Ciências Farmacêuticas Básica e Aplicada 31 (2010) 117–124.
[37] J.S.S. Quintans, E.W.M. Pereira, Y.M.B.G. Carvalho, P.P. Menezes, M.R. Serafini, M.V.A. Batista, C.D.L.F.A. Moreira, A.N.Á. Lima, A. Branco, J.R.G.S. Almeida, D.P. Gelain, G. Zengin, A.A.S. Araújo, L.J. Quintans-Júnior, Host-guest inclusion complexation of b-cyclodextrin and hecogenin acetate to enhance anti-hyperalgesic effect in an animal model of musculoskeletal pain, Process Biochem. 51 (2016) 1–9.
[38] N. Rajendiran, T. Mohandoss, G. Venkatesh, Investigation of inclusion complexes of sulfamerazine with α- and β-cyclodextrins: An experimental and theoretical study, Spectrochim. Acta A 124 (2014) 441–450, https://doi.org/10.1016/j.saa.2014.01.057.
[39] M. Kfoury, L. Auezova, S. Fourmentin, H. Greige-Gerges, Investigation of monoterpenes complexation with hydroxypropyl-β-cyclodextrin, J. Incl. Phenom. Macrocycl. Chem. (2014), https://doi.org/10.1007/s10847-014-0385-7.
[40] N.G. Hădărugă, D.I. Hădărugă, H.-D. Isengard, Water content of natural cyclodextrins and their essential oil complexes: a comparative study between Karl Fischer titration and thermal methods, Food Chem. 132 (4) (2012) 1741–1748.
[41] M.R. Serafini, P.P. Menezes, L.P. Costa, C.M. Lima, L.J. Quintans Jr., J.C. Cardoso, J.R. Matos, J.L. Soares-Sobrinho, S. Grangeiro Jr., P.S. Nunes, L.R. Bonjadim, A.A.S. Araújo, Interaction of p-cymene with β-cyclodextrin, J. Therm. Anal. Calorim. 109 (2012) 951–955.
[42] M. Jug, M. Becirevic-Lacan, Influence of hydroxypropyl-β-cyclodextrin complexation on piroxicam release from buccoadhesive tablets, Eur. J. Pharm. Sci. 21 (2004) 251–260.
[43] P.P. Menezes, G.A.A. Dória, A.A.S. Araújo, B.M.H. Sousa, L.J. Quintans-Júnior, R.N. Lima, P.B. Alves, F.M.S. Carvalho, D.P. Bezerra, F.J.B. Mendonça-Júnior, L. Scotti, M.T. Scotti, G.F. Silva, T.M. Aquino, A.R. Sabino, E.S.T. Egito, M.R. Serafini, Docking and physico-chemical properties of α- and β-cyclodextrin complex containing isopulegol: a comparative study, J. Incl. Phenom. Macrocycl. Chem. (2016), https://doi.org/10.1007/s10847-016-0633-0.
[44] M.S.S. Cunha-Filho, L.C.L. Sá-Barreto, Utilização de ciclodextrinas na formação de complexos de inclusão de interesse farmacêutico, Revista de Ciências Farmacêuticas Básica e Aplicada 28 (2007) 1–9.
[45] B. Pose-Vilarnovo, I. Perdomo-López, M. Echezarreta-López, P. Schroth-Pardo, E. Estrada, J.J. Torres-Labandeira, Improvement of water solubility of sulfamethizole through its complexation with β- and hydroxypropyl-β-cyclodextrin Characterization of the interaction in solution and in solid state, Eur. J. Pharm. Sci. 13 (2001) 325–331.
[46] G. Zhu, Z. Xiao, G. Zhu, Y. Niu Rujunzhou, Encapsulation of l-menthol in hydroxypropyl-β-cyclodextrin and release characteristics of the inclusion complex, Pol. J. Chem. Technol. 18 (3) (2016) 110–116.
[47] J.R. Moyano, J.M. Gines, M.J. Arias, A.M. Rabasco, Evaluation of dissolution characteristics of oxazepam-2-hydroxypropyl−/β-cyclodextrin binary systems, Pharm. Acta Helv. 69 (1994) 81–90.
[48] L.J. Yang, S.X. Ma, S.Y. Zhou, W. Chen, M.W. Yuan, Y.Q. Yin, X.D. Yang, Preparation and characterization of inclusion complexes of naringenin with β-cyclodextrin or its derivative, Carbohydr. Polym. 98 (2013) 861–869.
[49] S. Dou, Q. Ouyang, K. You, J. Qian, N. Tao, An inclusion complex of thymol into β-cyclodextrin and its antifungal activity against *Geotrichum citri-aurantii*, Postharvest Biol. Technol. 138 (2018) 31–36, https://doi.org/10.1016/j.postharvbio.2017.12.011.
[50] D.C. Sharma, R. Shukla, J. Ali, S. Sharma, P. Bajpai, N. Pathak, Phytochemical evaluation, antioxidant assay, antibacterial activity and determination of cell viability (j774 and thp1 αlpha cell lines) of *p. Sylvestris* leaf crude and methanol purified fractions, EXCLI J. 15 (2016) 85–94.
[51] E. Grela, A. Ząbek, A. Grabowiecka, interferences in the optimization of the mtt assay for viability estimation of *Proteus mirabilis*, Avicenna J. Med. Biotech. 7 (4) (2015) 159–167.
[52] M. Ijaz, J.A. Griessinger, A. Mahmood, F. Laffleur, A. Bernkop-Schnürch, Thiolated cyclodextrin: development of a mucoadhesive vaginal delivery system for acyclovir, J. Pharm. Sci. 105 (2016) 1714–1720.
[53] T. Mikami, K. Miyasaka, Effects of several anti-inflammatory drugs on the various parameters involved in the inflammatory response in rat carrageenin-induced pleurisy, Eur. J. Pharmacol. 95 (1983) 1–12.
[54] L.C. Loram, A. Fuller, T. Cartmell, B. Mitchell, D. Mitchell, Behavioural, histological and cytokine responses during hyperalgesia induced by carrageenan injection in the rat tail, Physiol. Behav. 92 (2007) 873–880.
[55] Y. Song, H. Zhao, J. Liu, C. Fang, R. Miao, Effects of citral on lipopolysaccharide-induced inflammation in human umbilical vein endothelial cells, Inflammation 39 (2) (2016) 663–671, https://doi.org/10.1007/s10753-015-0292-0.
[56] K. Hargreaves, R. Dubner, F. Brown, C. Flores, J. Joris, A new and sensitive method for measuring thermal nociception in cutaneous hyperalgesia, Pain 32 (1988) 77–88.
[57] I. Altun, Cytokine profile in degenerated painful intervertebral disc: variability with respect to duration of symptoms and type of disease, Spine J. Off. J. North Am. Spine Soc. 16 (2016) 857–861.
[58] Y. Chen, M.K. Boettger, A. Reif, A. Schmitt, N. Uçeyler, C. Sommer, Nitric oxide synthase modulates CFA-induced thermal hyperalgesia through cytokine regulation in mice, Mol. Pain 6 (2010) 13.
[59] P.S. Siqueira-Lima, A.M. Lucchese, H.G. Araújo-Filho, P.P. Menezes, A.A.S. Araújo, L.J. Quintans-Jr, J.S.S. Quintans, Inclusion of terpenes in cyclodextrins: preparation, characterization and pharmacological approaches, Carbohydr. Polym. 151 (2016) 965–987.
[60] R.G. Brito, A.A. Araújo, J.S. Quintans, K.A. Sluka, L.J. Quintans-Júnior, Enhanced analgesic activity by cyclodextrins - a systematic review and meta-analysis, Expert Opin. Drug Deliv. 12 (10) (2015) 1–12.
[61] G.F. Gebhart, K. Bielefeldt, Physiology of visceral pain, Compr. Physiol. 6 (4) (2016) 1609–1633.
[62] M.J. Millan, The induction of pain: an integrative review, Prog. Neurobiol. 57 (1) (1999) 1–164.
[63] J.C. Felipe, N.B.B. Graylin, H. Iandra, B.K. Juliana, E. Ricardo, D.O. Esther, S.F. Arturo, C.F. Valdir, L.M.Q. Nara, Anti-hyperalgesic effects of two sphingosine derivatives in different acute and chronic models of hyperalgesia in mice, Pharmacol. Rep. 70 (54) (2018) 753–759.